Visible-Infrared spectroscopy and chemical properties of water in mining area

Aliyeh Seifi, Mahdieh Hosseinjanizadeh, Hojjatolah Ranjbar
and Mehdi Honarmand

ABSTRACT

The present research focuses to investigate the relationship between spectral and chemical characteristics of water samples in Darrehzar mine. In order to reach this aim the chemical characteristics of water were measured through pH, electrical conductivity (EC) and inductively coupled plasma mass spectrometry (ICP-MS) analysis. Furthermore, the visible near infrared (VNIR) and shortwave infrared (SWIR) spectra of water samples were measured by Analytical Spectral Devices (ASD) FieldSpec^3 spectroradiometer and the relationships between spectral and chemical characteristics of water samples were calculated. Results of the pH and EC measurements showed that water with high acidity and EC values which indicates presence of acid drainage was located inside the mine. High concentration of copper, sulfur and iron at the samples could be related to copper mineralization and association with acid mine drainage. Results of spectroscopy revealed that second absorption feature (AF2) magnitude correlated significantly with pH (−0.599), EC (0.611) ($p < 0.1$) and total trace elements plus sulfur (0.822) ($p < 0.05$). The significant correlation of the AF2 magnitude with concentrations of S (0.854), Pb (0.914), Ni (0.836), Mn (0.834), Co (0.848) and AF3 with concentration of Fe (0.886) confirm that absorption feature magnitude increases by increasing metals concentrations in water.

Key words | absorption feature, chemical characteristics of water, darrehzar mine, field spectroscopy, pH and EC

Aliyeh Seifi
Mahdieh Hosseinjanizadeh (corresponding author)
Mehdi Honarmand
Department of Ecology, Institute of Science and High Technology and Environmental Sciences,
Graduate University of Advanced Technology,
Kerman,
Iran
E-mail: *m.hosseinjanizadeh@kgut.ac.ir*

Hojjatolah Ranjbar
Department of Mining Engineering,
Shahid Bahonar University,
Kerman,
Iran

INTRODUCTION

Water is a strong reactive material which can dissolves elements and objects when it moves through the porous media. The solubility of minerals increases in mining area due to the fractures. Fractured surfaces provide more exposed surface and that in turn causes more chemical reactions between water and the minerals. In the sulphidic mines, oxidation and dissolution of sulphide minerals such as pyrite, chalcopyrite and sphalerite raises hydrogen and sulphates in the water. As a result, water acidification occurs, water acidity increases and pH of water reduces (Blahwar 2010; Gyuris *et al.* 2010). Acidic water enables the dissolution of heavy metals so that with acidity raising the sulphates and metals concentrations will be increased in water.

An assessment on acidity values and environmental degradation were carried out in the Witwatersrand basin (South Africa) and Caveira abandoned mine (Southern Portugal) by temperature, H^+ activity (pH), oxidation-reduction potential (Eh), EC, electrical conductivity (EC), inductively coupled plasma (ICP) and ion chromatography (IC) measurements (Tutu *et al.* 2008; Ferreira da Silva *et al.* 2015). Furthermore, geochemical researches were performed in stream water, stream soil and stream sediments of Darrehzar mine (Iran) using pH, Eh, EC, AAS and inductively coupled plasma mass spectrometry (ICP-MS) in order to identify acid mine drainage pollution and determine trace metals and rare earth elements (Moor *et al.* 2012; Soltani *et al.* 2014).

doi: 10.2166/wst.2019.418

Spectroscopy which is one of the applicable methods in identification of ground materials, benefits from different parts of electromagnetic (EM) spectrum in material detection (van der Meer & de Jong 2006). Since water plays an important role in nature, water spectroscopy studies should be in priority in researches (Yamanouchi & Tanaka 1985; Buiteveld *et al.* 1994). A number of water researches focus on laboratory and mathematical studies for determining relationship between spectral absorption of water with temperature and salt dependencies in the ultraviolet, visible and infrared portions of EM spectrum (Sullivan *et al.* 2006; Wang 2008).

The spectral studies in the mining areas related to acid mine drainage (AMD) have been focused on reflectance spectral characterization of iron-oxide and sulphate minerals through field spectrometry and hyperspectral data (Anderson & Robbins 1998; Shi *et al.* 2014). In addition, some of studies focused on investigation of heavy metal concentration in deposits and vegetations of mining area (Choe *et al.* 2008; Li *et al.* 2008; Khalili *et al.* 2015). Mapping of heavy metal pollution in stream sediments using field spectroscopy revealed that variations in the spectral absorption features were linked to actual concentrations of heavy metals. So that, heavy metals concentrations in minerals increase absorption features depth at visible part (around 500 nm) and decrease absorption depth at shortwave infrared (SWIR) region (around 2,200 nm, where it is related to the OH bound in minerals) (Choe *et al.* 2008). Heavy metals accumulation in vegetation also can cause some effects such as increase the spectral reflectance, spectral shape blue-shift occurance, increase the red edge slope, decrease the chlorophyll and water absorption depth, the water absorption red-shift occurance and change the spectral profiles at the visible and near infrared portions (Li *et al.* 2008; Khalili *et al.* 2015).

Although spectral studies have been carried out for determination relationship between water absorption features with temperature and salinity of water as well as heavy metal levels in minerals and vegetation, the influence of heavy metals and pH in spectral properties of water in mining area have not been investigated yet. While increasing of heavy metals can cause environmental pollutants and affect on human health, applying these kinds of studies could be significant. Hence, in the present study, chemical properties of water in Darrehzar mine such as trace elements plus sulfur concentrations, pH and EC as well as spectral features of water samples were measured in order to investigate relationship between spectral characteristics in visible-infrared portion and chemical composition of water.

Study area

Darrehzar porphyry copper mine is located about 10 km south of the well-known Sarcheshmeh porphyry copper mine in Kerman province, southeast of Iran (Figure 1). The area has a moderate climate, with temperature ranges between −15°C (winter) and +33°C (summer), and annual precipitation from 300 to 500 mm. Darrehzar river with N-S direction intersected the mine into west and east parts. The river was permanent during the past with the discharge rate about 7 m^3/s at the end of winter and first days of spring. However, as a result of recent droughts, this river is not permanent and only in the wet seasons (winter and

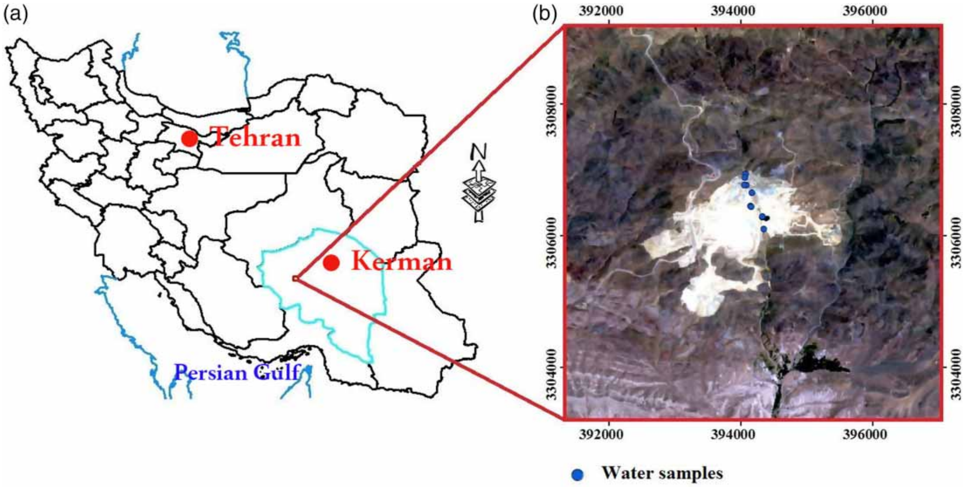

Figure 1 | (a) Location of the study area in Iran and Kerman province; (b) location of water samples which were plotted on Sentinel 2a image (Acquisition time: July 18, 2016).

spring) some springs are observed in the area (GSI 1973; Soltani *et al.* 2014).

The lithology of the area consists of Oligocene-Miocene dioritic and quartz dioritic bodies which were intruded into Eocene volcanic rocks compose mainly of volcanoclastics, andesite and trachyandesite rocks. Sericitic, silicic, chloritic, argillic and locally biotitic alterations are developed both in the intrusive bodies and in their host rocks. Three main fault systems have been recognized with an E-W (pre-mineralization fault), a NW-SE (mineralized fault) and a N-S striking (post-mineralization fault) in the Darrehzar deposit (GSI 1973; Ranjbar *et al.* 2000; Nateghi & Hezarkhani 2013; Hosseinjani Zadeh *et al.* 2014).

MATERIALS AND METHODS

Since normally different metal concentration were found in winter and summer seasons (Ferreira da Silva *et al.* 2015), water samples were collected from Darrehzar mine during two periods of field reconnaissance in winter and summer of 2016 in the present research. Eight water samples were collected from different part of the mine including; influx water to the mine (sample from surface water river named as Da31), near influx water to the mine (sample from surface water river named as Da22, Da29 and Da 30), groundwater in piezometer well in the mine (Da32), surface water lake in the eastern part of the mine (Da23-1), surface water pit lake in the western part of the mine (Da20-1), and discharging water from the mine (sample from surface water river named as Da24) in winter season (first field reconnaissance). However in the summer season (second field reconnaissance) influx and discharging water of the mine were dried and water table in piezometer well was fell down, so that only two water samples were collected including surface water lake in the eastern part of the mine (Da23-2) and surface water pit lake in the western part of the mine (Da20-2) (Table 1). Two samples were taken from each sampling points simultaneously. One was collected for EC, pH and spectroscopy analysis and the other which was acidified to $pH < 2$ with nitric acid (HNO_3) for measuring elements concentrations.

Water samples were collected by polyethylene bottles and their temperatures were recorded on-site. The collected water samples were transferred to Graduate University of Advanced Technology laboratory for EC, pH and spectroscopy measurements. The pH and EC of water samples were measured by Metrohm 827 lab pH meter and Metrohm 712 Conductometer EC meter. The spectroscopy analyses of the samples were conducted by ASD (Analytical Spectral Devices) FieldSpec$^{®3}$. Trace elements concentrations of acidic water samples were determined by ICP-MS using Agilent series 4,500 instrument. These samples were gathered from different part of mine including; surface water lake in the eastern part of the mine (Da23-1 and Da 23-2), surface water pit lake in the western part of the mine (Da20-1 and Da20-2), influx surface water river to the mine (Da31) and discharge surface water river from the mine (Da24). The elements concentrations and pH values were compared with standard values of drinking and natural mineral waters. In order to compare EC with standard values, first, EC was converted to total dissolved solids (TDS) by multiplying by an experimental coefficient (https://www.translatorscafe.com/

Table 1 | The geographic locations of water samples

Sampling date	Sample Number	Sampling site	Northing (UTM)	Easting (UTM)
08 March 2016	Da20-1	SWp in the western part of mine	3306444	394157
08 March 2016	Da22	SWr in the mine site	3306653	394170
08 March 2016	Da23-1	SWl in the eastern part of mine	3306288	394330
08 March 2016	Da24	SWr in the mine site (Downstream)	3306097	394347
08 March 2016	Da29	SWr in the mine site	3306773	394077
08 March 2016	Da30	SWr in the mine site	3306772	394051
08 March 2016	Da31	SWr in the mine site (Upstream)	3306942	394074
08 March 2016	Da32	GW (piezometer well) in the mine	3306885	394056
20 July 2016	Da23-2	SWl in the eastern part of mine	3306285	394327
20 July 2016	Da20-2	SWp in the western part of mine	3306453	394145

Abbreviations: GW: groundwater, SWr: Surface water river, SWl: Surface water lake, SWp: Surface water Pit Lake.

unit-converter/en-US/electric-conductivity/) and then TDS values was evaluated to standard values.

Noises were removed from spectra of water samples using ViewSpec Pro and SAMS (Spectral Analysis and Management System) software and magnitude of absorption features in spectra were analyzed with Equation (1) through SAMS software.

$$\alpha i = 1 - \frac{area\ under\ curve\ in\ [wp\ \&\ wq]}{area\ under\ line\ segment\ connecting\ si\ (wp)\ and\ si\ (wq)} \tag{1}$$

In this equation, αi is absorption feature analysis, *si* is absorption feature signature, *wp* is wavelength of maximum reflectance point before absorption feature and *wq* is wavelength of maximum reflectance point after absorption feature (Rueda & Wrona 2003).

The relationship between pH, EC and trace elements and sulfur concentrations (Al, As, Cd, Co, Cu, Fe, Mn, Mo, Ni, Pb, S, Sb and Zn) of water samples with absorption features analysis were determined through regression coefficient (R) and the significance threshold value were defined at 0.01, 0.05 and 0.1. The flowchart of the study procedure is shown in Figure 2.

RESULT AND DISCUSSION

Chemical properties

Results of chemical parameters of water samples showed that samples from surface water lake in the eastern part of the mine (Da23-1 and Da23-2) and surface water pit lake in the western part of the mine (Da20-1 and Da20-2) is characterized by low pH and high EC. The reason could be attributed to the situation of these samples which correspond to the phyllic alteration zone. Actually, this zone contains more than 10% pyrite and pyrite oxidation generates acid mine drainage (Costello 2003; Moor *et al.* 2012). Comparison of these samples (Da23-1, Da23-2, Da20-1 and Da20-2) with the maximum contaminant level (MCL) of pH and TDS for drinking water introduced by institute of standards and industrial research of Iran (ISIRI) revealed that the pH values of the samples were less than the MCL of pH however the TDS values were determined between the admissible limit (1,000 mg/l) and MCL (1,500 mg/l) (ISIRI 1053 2009). Moreover, pH levels of water in both places have reduced while EC and TDS have increased from winter to summer at these locations due to the heat and evaporation in summer which reduce the water content at the area. The TDS values of water samples from

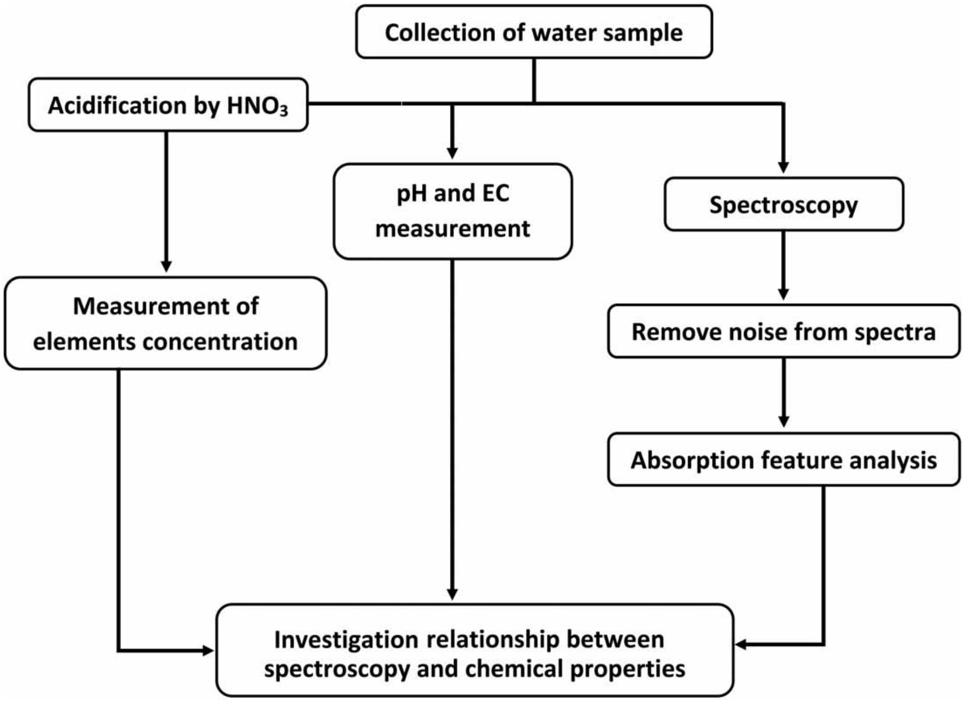

Figure 2 | Flowchart of the study procedure.

groundwater in piezometer well in the mine (Da32) and surface water river in bottom of the piezometer well in the mine (Da30) were also between the admissible limit (1,000 mg/l) and MCL (1,500 mg/l) of standard TDS (ISIRI 1053 2009) (Table 2).

Table 2 | pH, EC and TDS for the water samples

Sample name	**pH**	**EC (μs/cm)**	**TDS (ppm)**
MCL	6.5–9	–	1,500
Da20-1	3.48	1,570	1,004.8
Da22	8.09	484.4	310.016
Da23-1	4.28	1,583	1,013.12
Da24	7.88	582.5	372.8
Da29	6.6	645.8	413.312
Da30	7.43	1,948	1,246.72
Da31	7.9	453.7	290.368
Da32	7.23	1,991	1,274.24
Da23-2	3.18	2,218	1,419.52
Da20-2	2.75	2,247	1,438.08

Abbreviation: MCL: Maximum Contaminant Level

In addition, elements such as; Al, As, Cd, Co, Cr, Cu, Fe, Mn, Mo, Ni, Pb, S, Sb and Zn were analyzed using ICP-MS. Result of ICP-MS shows that Al, Cu, Fe, Mn, S and Zn (mg/l) concentrations were higher than other elements (Figure 3). S, Cu and Al occupy the most levels which can be attributed to the association with sulfuric copper mineralization and aluminium bearing minerals such as plagioclase crystals in the quartz monzonitic body (Darrehzar porphyry) (Soltani *et al.* 2014; Ravankhah *et al.* 2009). High concentration of Fe and Mn may have derived from pyrite oxidation and high Fe and S values in water samples probably referred to presence of acidic mine drainage. The analysis revealed that trace elements such as Al, Fe, Mn and S; are significantly enriched in acid water and vary seasonally as increased from winter to summer in the mine. This situation also was observed at the study implemented by Ferreira da Silva *et al.* (2015). Furthermore concentration of the elements (except Mo) in acidic water at the inside of the mine including; surface water lake in the eastern part of the mine (Da23) and surface water pit lake in the western part of the mine (Da20) were much more than neutral water from the influx and discharging water of the mine. This can be arisen from the fact that Mo has a different

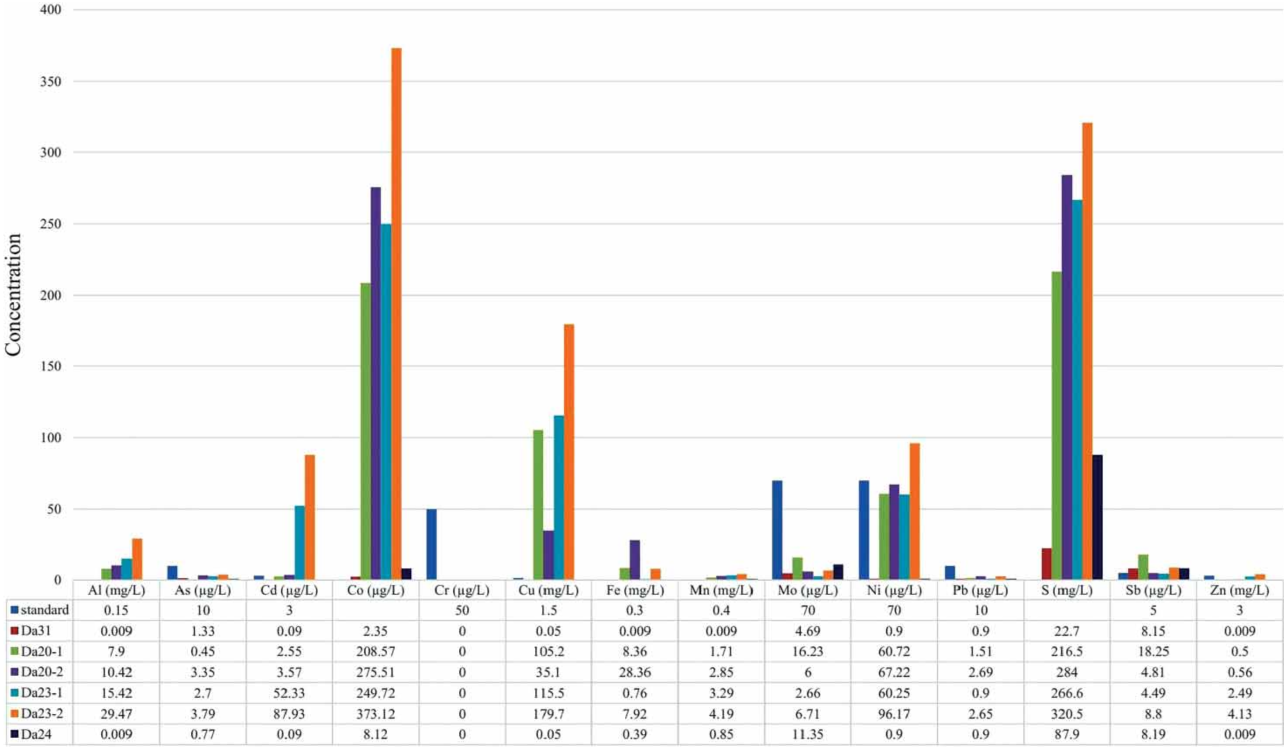

	Al (mg/L)	As (μg/L)	Cd (μg/L)	Co (μg/L)	Cr (μg/L)	Cu (mg/L)	Fe (mg/L)	Mn (mg/L)	Mo (μg/L)	Ni (μg/L)	Pb (μg/L)	S (mg/L)	Sb (μg/L)	Zn (mg/L)
■ standard	0.15	10	3		50	1.5	0.3	0.4	70	70	10		5	3
■ Da31	0.009	1.33	0.09	2.35	0	0.05	0.009	0.009	4.69	0.9	0.9	22.7	8.15	0.009
■ Da20-1	7.9	0.45	2.55	208.57	0	105.2	8.36	1.71	16.23	60.72	1.51	216.5	18.25	0.5
■ Da20-2	10.42	3.35	3.57	275.51	0	35.1	28.36	2.85	6	67.22	2.69	284	4.81	0.56
■ Da23-1	15.42	2.7	52.33	249.72	0	115.5	0.76	3.29	2.66	60.25	0.9	266.6	4.49	2.49
■ Da23-2	29.47	3.79	87.93	373.12	0	179.7	7.92	4.19	6.71	96.17	2.65	320.5	8.8	4.13
■ Da24	0.009	0.77	0.09	8.12	0	0.05	0.39	0.85	11.35	0.9	0.9	87.9	8.19	0.009

Figure 3 | Concentration of trace elements and sulfur in the water samples of Darrehzar mine (Da31: surface water river in the mine site (Upstream); Da20-1 and Da20-2: surface water pit lake in the western part of mine; Da23-1 and Da23-2: surface water lake in the eastern part of mine; Da24: surface water river in the mine site (Downstream)).

geochemical behavior in acidic condition and is insoluble in low pH values (Moor *et al.* 2012; Soltani *et al.* 2014). In addition, higher concentrations of Al, As, Cd, Co, Cu, Mn, S, Ni and Zn were observed in water samples from surface water lake in the eastern part of the mine. While highest concentrations of Fe, Mo, Pb and Sb were observed in surface water samples from pit lake in the western part of the mine especially at the summer (Figure 3). The values of Mn, Co and Ni from the surface water lake ($pH = 4.28$ in winter and 3.18 in summer) are more than the values for these elements in the surface water pit lake ($pH = 3.48$ in winter and 2.75 in summer) while Fe concentration was higher at the surface water pit lake. This can be attributed to geochemical behavior of these elements so that Fe precipitates at lower pH relative to Mn, Cr, Co and Ni. It also should be notice that Al, Cd, Cu, Fe, Mn, Ni, Sb and Zn levels exceeded from the defined MCL determined by World Health Organization (WHO 2011), Codex Standard 108 (1981) and institute of standards and industrial research of Iran (ISIRI 2441 2004; ISIRI 1053 2009) (Figure 3). There is no defined MCL level for cadmium (Cd) and sulfur (S) by WHO, Codex Standard and ISIRI for drinking and natural mineral water.

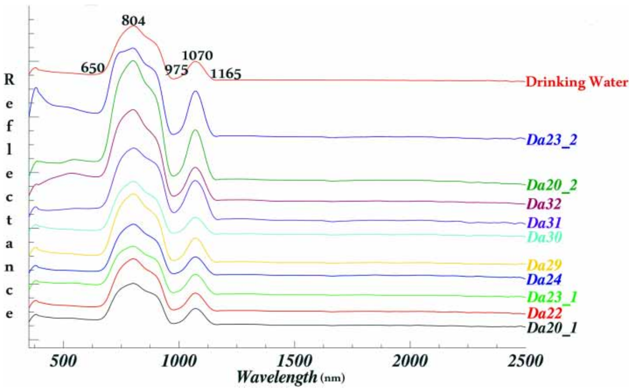

Figure 4 | Spectra of collected water samples from Darrehzar mine; the first absorption feature (AF1) located in 650 nm, the second absorption feature (AF2) in 975 nm and the third absorption feature (AF3) in 1,165 nm.

Absorption features

Spectral measurements were carried out for all of samples as well as drinking water (Figure 4). Result of spectroscopy showed that the water spectra were similar with negligible differences. So that three absorption features at the 650, 975 and 1,165 nm and two reflectance peaks at 804 and 1,070 nm can be observed in water spectra. The absorption features relatively corresponds with the results stated in Tanaka and Yamanouchi (1985) which measured and estimated water vapor (H_2O) absorptions in VNIR at 900 and 1,100 nm. In addition, Sullivan *et al.* (2006) stated an absorption feature in 662 nm for water with temperature dependency.

The magnitude of three absorption features at 650, 975 and 1,165 nm which were indicated by AF1, AF2 and AF3 respectively were determined using Equation (2) (Figure 5). Result of absorption feature analysis illustrated that drinking water contains higher values of absorption magnitudes than Darrehzar water samples at all absorption features except the second absorption feature of Da23-2. In addition,

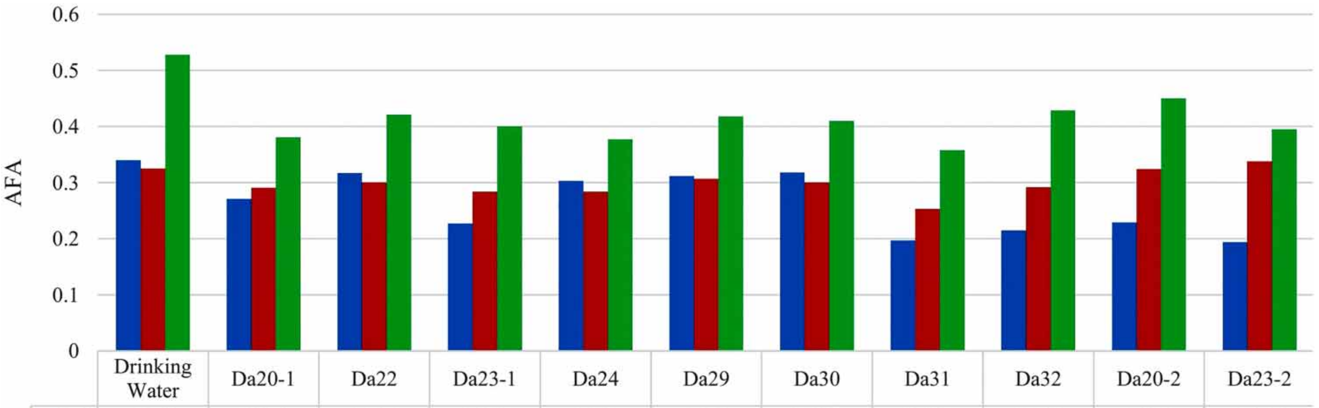

	Drinking Water	Da20-1	Da22	Da23-1	Da24	Da29	Da30	Da31	Da32	Da20-2	Da23-2
🟦 AF1	0.34	0.271	0.317	0.227	0.303	0.312	0.318	0.197	0.215	0.229	0.194
🟥 AF2	0.325	0.291	0.3	0.284	0.284	0.307	0.3	0.253	0.292	0.324	0.338
🟩 AF3	0.528	0.381	0.421	0.4	0.377	0.418	0.41	0.358	0.429	0.45	0.395

Figure 5 | Result of absorption feature analysis (AFA) in water spectra (Da20-1 and Da20-2: Surface water pit lake in the western part of mine; Da22: Surface water river in the mine site; Da23-1 and Da23-2: Surface water lake in the eastern part of mine; Da24: Surface water river in the mine site (Downstream); Da29: Surface water river in the mine site; Da30: Surface water river in the mine site; Da31: Surface water river in the mine site (Upstream); Da32: groundwater (piezometer well) in the mine).

comparison of the results revealed that the influx water to the mine (Da31) contains the least values and this sample had the least levels of EC and dissolved metal as well (Figure 5 and Table 2). The amount of absorption magnitude for third absorption feature for all samples is more than the two other absorption features. The second absorption features magnitudes of acidic water (Da20-1, Da20-2, Da23-1 and Da23-2), water with colloids (Da32) and surface water river in the upstream (Da31) is bigger than the first absorption features magnitudes and vice versa for other water samples (Da22, Da24, Da29 and Da30) (Figure 5). The samples with higher EC such as Da20-2, Da23-2 and Da32 presented more differences between the first and second absorption features. However, it is not accurate for Da30 (high EC and low difference) and Da31 (low EC and high difference). This shows that besides EC other processes such as presence of elements and colloids could be influence on the spectral characteristics.

Furthermore, comparison of spectra in Figure 4 showed that absorption value is reduced in the spectra of acidic water such as Da20 and Da23 and they represent a small reflectance at 548 and 518 nm, respectively (Figure 6(a)). This probably is associated with dissolved particles e.g. Cu bearing compositions in water samples. Referring to the field studies and the ICP results, presence of chalcanthite ($CuSO_4$. $5H_2O$) and high content of Cu and S in the site

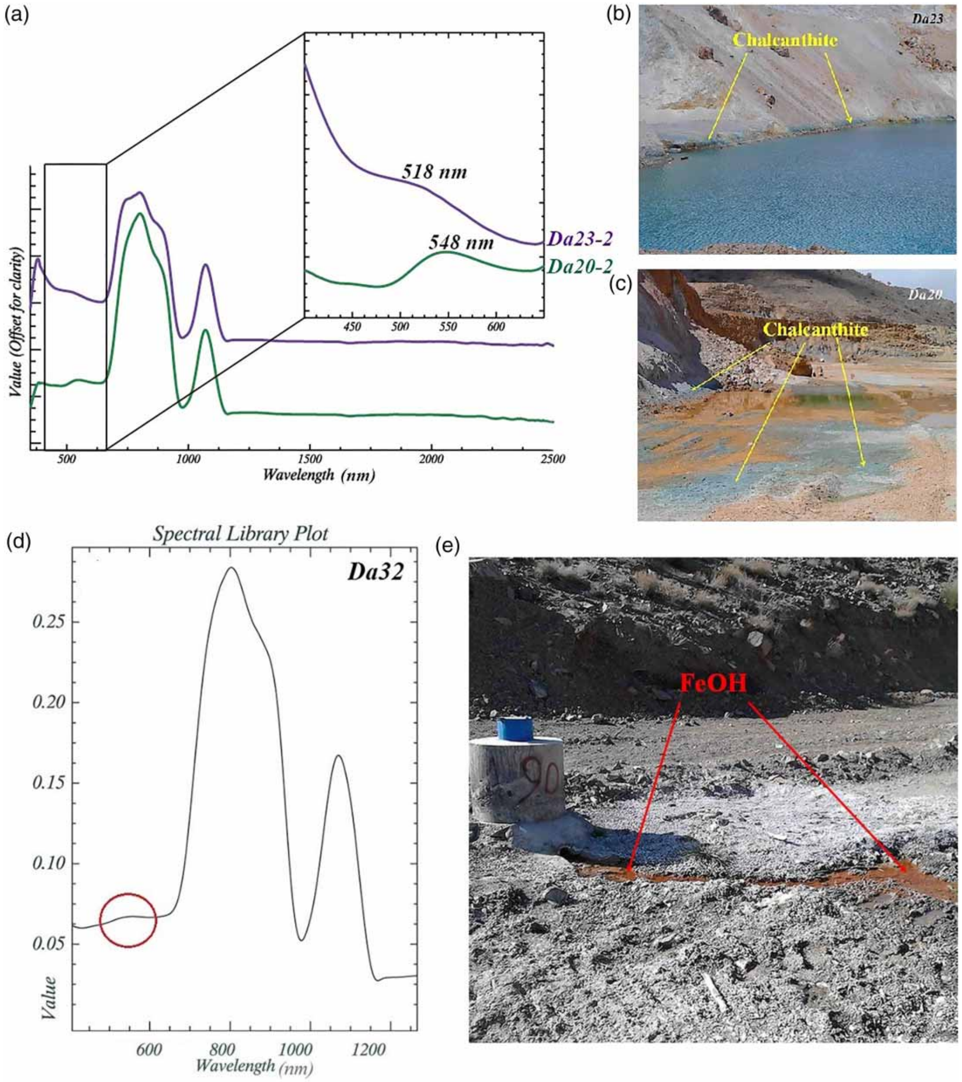

Figure 6 | (a) Spectra of acidic water and their small reflectances at 548 and 518 nm; (b) Presence of chalcanthite in Surface water lake in the eastern part of the mine (Da23); (c) Presence of chalcanthite in Surface water pit lake in the western part of the mine (Da20); (d) A broad small reflectance in 546-525 nm of Da32 spectrum (reflectance is situated by circle); (e) the piezometer well and FeOH sediments in its stream.

of acidic water (surface water lake in the eastern part and surface water pit lake in the western part of the mine), reflecting the fact that $CuSO_4$ particles are in dissolved state in the water (Figures 3, 6(b) and 6(c)). In addition, a broad small reflectance is seen at 546–525 nm in spectra of Da32 which have been taken from the piezometer well in the mine (Figure 6(d)). Fe-bearing precipitations downstream from the piezometer well probably reflected presence of colloids in the water and creating the reflectance (Figure 6(e)). Furthermore, the first absorption feature value for acidic water and water of piezometer well with colloids was less than the first absorption feature of other samples.

Relationship between absorption features and chemical properties

Table 3 presents regression (R^2), equation for calculating regression, and correlation (R) between the magnitudes of absorption features with EC and pH parameters. The first absorption feature correlates positively with pH (0.462) and negatively with EC (−0.425) and vice versa for both of the second and third absorption features (Table 3). The second absorption feature displays a significant correlation with pH (−0.599) and EC (0.611) ($p < 0.1$). This region (975 nm) is corresponding with the results of Estifanos (2006) which determined the absorption features related to pH and EC in 852–1,036 nm.

Total elements concentrations (Al, As, Cd, Co, Cu, Fe, Mn, Mo, Ni, Pb, S, Sb and Zn) show a negative correlation with the first absorption feature and a positive correlation with both the second and the third absorption features (Figure 7). The second absorption feature correlated significantly with total elements ($R = 0.822$; $p < 0.05$) (Figure 7(b)). Regressions between total elements with pH and EC were also computed and show significant relationship ($R = 0.94$ for pH and $R = 0.93$ for EC) ($p < 0.01$) (Table 3). It referred that pH and EC parameters can be influence on trace elements solution. Thus, dissolved metal concentration rises in water while an increase in EC and a decrease of pH occurred which confirmed by Anderson (1994), Tutu *et al.* (2008) and Soltani *et al.* (2014).

Table 3 | Regression (R^2) and correlation (R) between absorption features magnitudes and total elements with EC and pH parameters

		Equation	R^2	R
pH	AF1	$y = 0.0108x + 0.1948$	0.214	0.462
	AF2	$y = -0.0064x + 0.3348$	0.359	0.599
	AF3	$y = -0.0021x + 0.4162$	0.028	0.167
EC	AF1	$y = -3E\text{-}05x + 0.2983$	0.181	0.425
	AF2	$y = 2E\text{-}05x + 0.2713$	0.373	0.611
	AF3	$y = 2E\text{-}05x + 0.3814$	0.204	0.451
pH	Total elements	$y = -79.59x + 685.1$	0.8906	0.943716**
EC	Total elements	$y = 0.2403x\text{-}52.38$	0.8746	0.935201**

**$p < 0.01$.

There is a significant correlation between the second absorption feature and Co, Mn, Ni, Pb and S ($p < 0.05$) (Figure 8). According to the ICP-MS results Al, Cu, Mn, S and Zn indicated high concentration in water samples (Figure 3). Gupta (2003) stated that spectral characteristics in the VNIR part of the EM spectrum are dominated by electronic processes in transition metals (e.g. Fe, Mn, Cu, etc.) and the electronic processes in transition Cu occur in 800 nm. This region is situated between the first (650 nm) and second (975 nm) absorption features of water spectra. In addition, Estifanos (2006) introduced the 996–1,163 nm region as an indicator spectral region to predict Mn in polluted mining area by partial least square regression (PLSR) technique. This region is also located between the second and third (1,165 nm) absorption features of water spectra. Furthermore, the indicator spectral regions in 573–765 nm and 873–1,101 nm were presented for Zn recognition using PLSR technique (Estifanos 2006). Both regions conform to the first and second absorption features of water spectra as a result, regression value of these two absorption features are close. Fe which has high concentration shows a significant correlation with the third absorption feature. There are crystal field transitions of ferric iron in 550–650 nm and 750–950 nm as well as in 900–1,100 nm for ferrous iron (Zabcic 2008). The electronic transition of ferrous iron conforms to the third absorption feature (Figure 8).

CONCLUSION

Results of the pH and EC measurements showed that water with low pH, high EC and high concentrations of trace elements and S was located inside the mine and water with high pH, low EC and low concentrations of the elements was situated in the influx and discharging parts of the mine. Moreover, the collected water samples in summer displayed lower pH, higher EC and dissolved metals than water samples of winter season. Large amounts of copper and sulfur in water samples could be related to copper mineralization in phyllic alteration zone. Furthermore water with low pH, high iron and sulfur concentrations were associated with phyllic zone and this condition normally happen due to the oxidation of pyrite

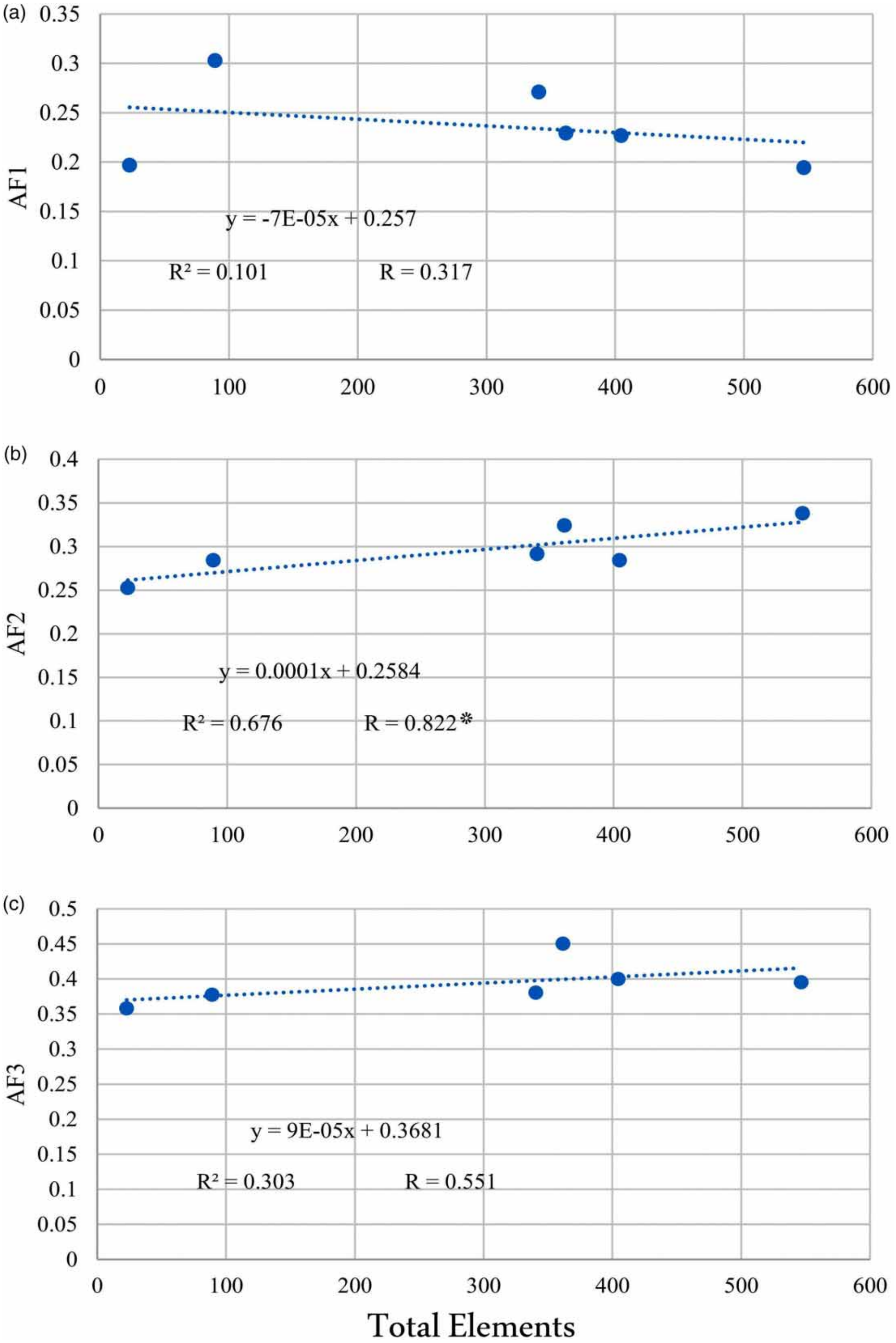

Figure 7 | (a) the relationship between the first absorption feature with total elements; (b) the relationship between the second absorption feature with total elements; (c) the relationship between the third absorption feature with total elements (*$p < 0.05$).

and producing acid mine drainage. Results of spectroscopic studies presented similar spectra for water samples that contain three absorption features in visible-near infrared region. The second absorption feature (AF2) magnitude correlated significantly with total elements (0.822) ($p < 0.05$). The close correlation between the AF2 magnitude with S (0.854), Pb (0.914), Ni (0.836), Mn (0.834), Co (0.848) concentrations and third absorption feature (AF3) magnitude

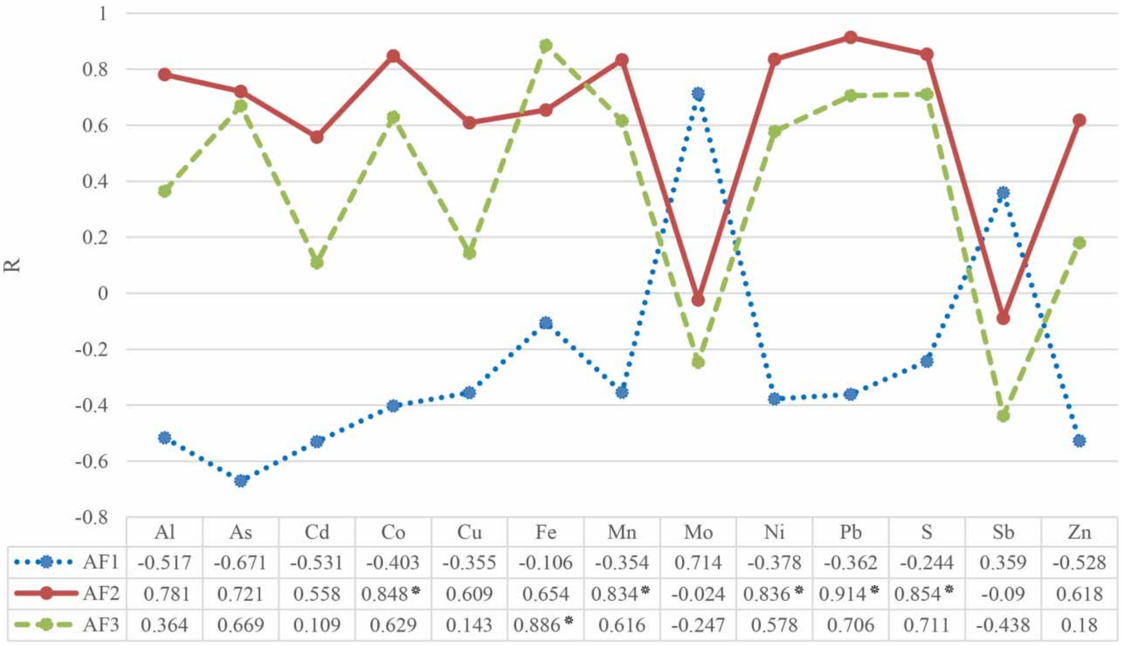

	Al	As	Cd	Co	Cu	Fe	Mn	Mo	Ni	Pb	S	Sb	Zn
AF1	-0.517	-0.671	-0.531	-0.403	-0.355	-0.106	-0.354	0.714	-0.378	-0.362	-0.244	0.359	-0.528
AF2	0.781	0.721	0.558	0.848*	0.609	0.654	0.834*	-0.024	0.836*	0.914*	0.854*	-0.09	0.618
AF3	0.364	0.669	0.109	0.629	0.143	0.886*	0.616	-0.247	0.578	0.706	0.711	-0.438	0.18

Figure 8 | The correlation (R) between the elements concentrations with absorption feature magnitudes of water spectra (*$p < 0.05$.).

with Fe (0.886) concentration showed that the magnitude of absorption feature increases when the elements concentrations increase in water. However changes in the magnitude of absorption feature is negligible compare to changes the elements. Although the results show that trace elements and S concentrations, EC and pH can effect on the spectral properties of water and there is correlation between them, much effort remain to be done in other areas and more samples for verifying accurate determination and investigation of colloidal particles (e.g. FeOH and $CuSO_4$) affects.

ACKNOWLEDGEMENTS

The authors are sincerely grateful to the geologists and staff of the Sarcheshmeh and Darrehzar copper mines for providing the facilities and kindly helping us during our field work and sample collection.

REFERENCES

Anderson, J. 1994 Spectral characterization of acid-mine and neutral-drainage bacterial precipitates and their relationship to water quality in a piedmont watershed. *Virginia Journal of Science* **45**, 175–186.

Anderson, J. & Robbins, E. 1998 Spectral reflectance and detection of iron-oxide precipitates associated with acidic mine drainage. *Photogrammetric Engineering & Remote Sensing* **64**, 1201–1208.

Blahwar, B. 2010 *Identification of the Extent of Artisanal Coal Mining and Related Acid Mine Water Hazards Using Remote Sensing and Field Sampling A Case Study in Jaintia Hills of North-Eastern India*. M.Sc dissertation, International Institute for Geo-information Science and Earth Observation, Enschede, the Netherlands and the Indian Institute of Remote Sensing, Dehradun, India.

Buiteveld, H., Hakvoort, J. H. M. & Donze, M. 1994 The optical properties of pure water. *SPIE* **2258** (Ocean Optics XII), 174–183.

Choe, E., Meer, F., Ruitenbeek, F., Werff, H., Smeth, B. & Kim, K. W. 2008 Mapping of heavy metal pollution in stream sediments using combined geochemistry, field spectroscopy, and hyperspectral remote sensing: a case study of the Rodalquilar mining area, SE Spain. *Remote Sensing of Environment* **112**, 3222–3233.

Codex Standard 108. 1981 *CODEX Standard for Natural Mineral Waters*.

Costello, C. 2003 *Acid Mine Drainage: Innovative Treatment Technologies*. National Network of Environmental Management Studies Fellow for U.S. Environmental Protection Agency, Washington.

Estifanos, S. 2006 *Spectral Indicators for Assessing Pollution in the Epithermal Gold Mining Area of Rodalquilar, SE Spain*. M.S dissertation, International Institute for Geo-information Science and Earth Observation, Enschede, Netherlands.

Ferreira da Silva, E., Durães, N., Reis, P., Patinha, C., Matos, J. & Costa, M. R. 2015 An integrative assessment of environmental degradation of Caveira abandoned mine area (Southern Portugal). *Journal of Geochemical Exploration* **159**, 33–47.

Geological Survey of Iran (GSI) 1973 *Exploration for ore Deposit in Kerman Region*. Geological Survey of Iran Report Y/53, Tehran.

Gupta, R. P. 2003 *Remote Sensing Geology. Second Edition ed*. Springer-Verlag Berlin Heidelberg, New York.

Gyuris, P., Tote, C., Reusen, I., Delalieux, S. & Kolodyazhnyy, O. 2010 *WP4-Satellite Remote Sensing, Deliverable D4.1, Report on the Limitations and Potentials of Satellite EO Data*. GEONARDO Environmental Technologies Ltd, Hungary.

Hosseinjani Zadeh, M., Tangestani, M. H., Velasco Roldan, F. & Yusta, I. 2014 Spectral characteristics of minerals in alteration zones associated with porphyry copper deposits in the middle part of Kerman copper belt, SE Iran. *Ore Geology Reviews* **62**, 191–198.

ISIRI 1053 2009 *Drinking Water-Physical and Chemical Specifications*, 5th revision ed. Institute of Standards and Industrial Research of Iran.

ISIRI 2441 2004 *Natural Mineral Water – Specifications*, First eddition ed. Institute of Standards and Industrial Research of Iran.

Khalili, R., Anvari, S. & Honarmand, M. 2015 Combination of Biochemical and Hyperspectral Remote Sensing Methods for Detection of Heavy Metal Pollutions in Eucalyptus Leaves (Case Study: The City of Bam). In: *International Conference on Sensors & Models in Remote Sensing & Photogrammetry, Kish Island, Iran*.

Li, Q., Yang, F., Zhang, B., Zhang, X. & Zhou, G. 2008 Biogeochemistry responses and spectral characteristics of Rhus Chinensis Mill under heavy metal contamination stress. *Journal of Remote Sensing* **12** (2), 284–290.

Moor, F., Soltani, N., Keshavarzi, B., Esmaeel Zadeh, A. & Karimi, M. 2012 Environmental geochemistry of water, soil, and sediments in Darrehzar copper deposit (Kerman). *Journal of Advanced Applied Geology* **3**, 29–37.

Nateghi, A. & Hezarkhani, A. 2013 Fluid inclusion evidence for hydrothermal fluid evolution in the Darreh-Zar porphyry copper deposit, Iran. *Journal of Asian Earth Sciences* **73**, 240–251.

Ranjbar, H., Roonwal, G. S., Ravindran, K. V. & Babar, S. 2000 Synergetic use of remote sensing and geophysical data for exploration of porphyry copper deposits, using GIS. *Journal of the Indian Society of Remote Sensing* **28** (2&3), 205–212.

Ravankhah, A., Moaiyad, M., Amini, S. & Hossein Zadeh, G. 2009 Discussion of geology, petrology, economic geology and alteration zones in Darrehzar porphyry copper deposit (South West of Kerman). *Journal of Geological Survey of Iran* **12**, 63–75.

Rueda, C. A. & Wrona, A. F. 2003 *Spectral Analysis and Management System, User's Manual*, Version 2.0 ed. University of California, Davis, California.

Shi, X., Aspandiar, M. & Oldmeadow, D. 2014 Reflectance spectral characterization and mineralogy of acid sulphate soil in subsurface using hyperspectral data. *International Journal of Sediment Research* **29**, 149–158.

Soltani, N., Moore, F., Keshavarzi, B. & Sharifi, R. 2014 Geochemistry of trace metals and rare earth elements in stream water, stream sediments and acid mine drainage from darrehzar copper mine, Kerman, Iran. *Water Qual Expo Health* **6**, 97–114.

Sullivan, J. M., Twardowski, M. S., Zaneveld, J. R., Moore, C. M., Barnard, A. H., Donaghay, P. L. & Rhoades, B. 2006 The hyperspectral temperature and salt dependencies of absorption by water and heavy water in the 400–750 nm spectral range. *Applied Optics* **45**, 5294–5309.

Tutu, H., McCarthy, T. S. & Cukrowska, E. 2008 The chemical characteristics of acid mine drainage with particular reference to sources, distribution and remediation: the Witwatersrand Basin, South Africa as a case study. *Applied Geochemistry* **23**, 3666–3684.

van der Meer, F. D. & de Jong, S. M. 2006 *Imaging Spectrometry, Basic Principles and Prospective Applications*. Springer, Dordrecht, The Netherlands.

Wang, L. 2008 *Measuring Optical Absorption Coefficient of Pure Water in UV Using the Integrating Cavity Absorption Meter*. PhD thesis, Texas A&M University.

WHO 2011 *Guidelines for Drinking-Water Quality*, 4th edn. World Health Organization.

Yamanouchi, T. & Tanaka, M. 1985 Absorption properties of the near-infrared water vapor bands. *Journal of Quantitative Spectroscopy and Radiative Transfer* **34** (6), 463–472.

Zabcic, N. 2008 *Derivation of Surface pH-Values Based on Mineral Abundances Over Pyrite Mining Areas with Airborne Hyperspectral Data (Hymap) of Sotiel-Migollas Mine Complex, Spain. M.S dissertation*, University of Alberta, Edmonton.

First received 24 June 2019; accepted in revised form 29 November 2019. Available online 20 December 2019